TEV protease-facilitated stoichiometric delivery of multiple genes using a single expression vector

Xi Chen,[1] Elizabeth Pham,[1] and Kevin Truong[1,2]*

[1]Institute of Biomaterials and Biomedical Engineering, University of Toronto, 164 College Street, Toronto, Ontario, M5S 3G9, Canada

[2]Edward S. Rogers Sr. Department of Electrical and Computer Engineering, University of Toronto, 10 King's College Circle, Toronto, Ontario, M5S 3G4, Canada

Received 3 June 2010; Revised 27 September 2010; Accepted 29 September 2010
DOI: 10.1002/pro.518
Published online 13 October 2010 proteinscience.org

Abstract: Delivery and expression of multiple genes is an important requirement in a range of applications such as the engineering of synthetic signaling pathways and the induction of pluripotent stem cells. However, conventional approaches are often inefficient, nonstoichiometric and may limit the maximum number of genes that can be simultaneously expressed. We here describe a versatile approach for multiple gene delivery using a single expression vector by mimicking the protein expression strategy of RNA viruses. This was accomplished by first expressing the genes together with TEV protease as a single fusion protein, then proteolytically self-cleaving the fusion protein into functional components. To demonstrate this method in *E. coli* cells, we analyzed the translation products using SDS-PAGE and showed that the fusion protein was efficiently cleaved into its components, which can then be purified individually or as a binding complex. To demonstrate this method in mammalian cells, we designed a differential localization scheme and used live cell imaging to observe the distinctive subcellular targeting of the processed products. We also showed that the stoichiometry of the processed products was consistent and corresponded with the frequency of appearance of their genes on the expression vector. In summary, the efficient expression and separation of up to three genes was achieved in both *E. coli* and mammalian cells using a single TEV protease self-processing vector.

Keywords: TEV protease; polycistronic protein expression; fusion proteins; live cell imaging

Introduction

The ability to introduce multiple genes into cells is essential for a wide range of applications, for example, the co-delivery of reporter or suicide genes, the assembly of multiprotein complexes,[1] the engineering of synthetic signaling pathways,[2] and the induction of pluripotent stem cells.[3] Conventionally, multiple genes can be expressed in a cell through simultaneous or sequential transfections of multiple vectors. However, this method becomes tedious and inefficient as the number of vectors increases. The expression of multiple genes from a single vector can be achieved by incorporating expression cassettes each with its own independent promoter. Unfortunately, this method is susceptible to gene suppression as a result of promoter interference.[4] The internal ribosomal entry site mediated polycistronic vector is an improvement to the aforementioned multiple expression vector as it expresses all its

Additional Supporting Information may be found in the online version of this article.

Grant sponsor: The Canadian Institutes of Health Research; Grant number: #81262; Grant sponsor: Heart and Stroke Foundation; Grant number: #NA6241.

*Correspondence to: Kevin Truong, Institute of Biomaterials and Biomedical Engineering, University of Toronto, 164 College Street, Toronto, Ontario, M5S 3G9, Canada. E-mail: kevin.truong@utoronto.ca

genes from a single open reading frame through a translation reinitiation mechanism.[5] However, the translations are uncoupled in the sense that they are invoked from different translational initiation events. Consequently, the proteins are not produced in stoichiometric proportions, with a heavier bias on upstream expression.[6] To achieve stoichiometric expression of multiple genes using a single expression vector, 2A sequences from picornaviruses have been used because they can disrupt the formation of the peptide bond during protein synthesis.[1,7–9] The 2A sequences, however, has not been shown to work in bacterial cells,[10] widely vary in their efficiency of peptide bond disruption[11,12] and leave long residual trailing sequences (20–30 residues) to proteins that may perturb their function. Furthermore, in the case of some proteins targeted to the exocytic pathway, the cellular localization of proteins downstream of the 2A sequences were dictated by their upstream partners.[13]

In this study, we developed a multiple gene expression system that instead mimics the proteolytic processing of polyproteins found in tobacco etch viruses (TEVs) of the Potyviridae family.[14] TEVs express all of their proteins in the form of polyproteins before they are processed by the TEV nuclear inclusion α protease (TEV protease).[15,16] TEV protease is able to cleave its substrate ENLYFQS between QS with high specificity, leaving a 6-residue on the upstream protein and a single Ser residue on the downstream protein.[17] TEV protease is widely used in purification strategies to separate the passenger proteins from affinity tags.[18–20] Several studies also utilized TEV protease in eukaryotes to cleave engineered fusion proteins and study subsequent biological effects.[21–24] However, TEV protease has mostly been expressed separately from the fusion protein that it cleaves. To achieve genuine single vector transfection, TEV protease can be delivered with the genes of interest as a fusion, requiring TEV protease to "self-cleave" within the same molecule. TEV protease self-cleavage was first demonstrated in plant cells,[25] but has only once been utilized to separate two proteins expressed from *E. coli* cells.[26] We expanded the utility of TEV protease self-cleavage by demonstrating the efficient and stoichiometric separation of up to three functionally intact proteins in both bacterial (*E. coli*) and mammalian cells. In doing so, we have introduced a versatile approach for the correlated expression of multiple gene products from a single vector.

Results and Discussion

Characterization of the TEV protease (TEVp)

The TEVp we used was a variant developed by Kapust *et al.* which contains a S291V mutation.[27] This mutation has been shown to reduce TEVp autoproteolysis and in turn enhance its proteolytic activity on canonical substrates.[27,28] To confirm the activity of this TEVp, we constructed a fluorescence resonance energy transfer (FRET) sensor, Ven-tevS-Ceru consisting of the TEVp substrate tevS (ENLYFQS) flanked by the acceptor Venus (YFP variant[29]) and the donor Cerulean (enhanced CFP[30]). We also constructed a control sensor, Ven-linker-Ceru, with the TEV substrate tevS replaced by an arbitrary linker (DAPVRSLNCT). We conducted the activity assay *in vitro* by mixing Venus-tagged TEVp (TEVpVen) and the sensors in a 1:1 ratio. The cleavage of the Ven-tevS-Ceru sensor was immediately observed by a gradual decline in FRET efficiency (Supporting Information Fig. S1). In contrast, Ven-linker-Ceru remains unchanged in the experimental time frame of 40 min.

TEVp expression has been previously shown to be nontoxic in *E. coli,*[31] yeast,[32] *Drosophila,*[22] and mammalian cells.[33] To confirm this, we expressed TEVp in COS-7, HeLa, and HEK-293 cells. Cell morphologies were unaffected, and the expression of TEVpVen was robust with distribution in the cytoplasm, nucleus, and nucleolus of the cell. This indicates the unlikelihood for the existence of endogenous TEVp substrates in these cell types and establishes the crucial prerequisite for using TEVp as a tool in basic biology research.

TEVp self-cleavage in E. coli *bacteria*

The TEVp self-cleavage of fusion proteins in *E. coli* effectively expressed multiple proteins which could then be purified individually or in protein complexes. TEVp self-cleavage refers to the cleavage of TEVp substrates residing on the same molecule as TEVp itself. The mode of interaction between TEVp and its substrate in self-cleavage events can be both intermolecular and intramolecular. Intramolecular cleavages are more efficient due to the closer proximity between the TEVp active site and its substrate, albeit only possible in cases where the substrate can be accessed by the active site through molecular bending and rotation. A natural example of intramolecular TEVp self-cleavage is the autoproteolysis of wild-type TEVp between residues 218 and 219.[27,28]

As an initial test for TEVp self-cleavage, TEVp was fused to the N-terminal of both Ven-tevS-Ceru and the control sensor Ven-linker-Ceru, creating TEVp-tevS-Ven-tevS-Ceru and TEVp-tevS-Ven-linker-Ceru respectively. FRET measurements were taken after 1 day of expression in *E. coli* cells. The FRET ratio (Venus/Cerulean) in cells expressing TEVp-tevS-Ven-linker-Ceru was 2.08 ± 0.13 ($n = 3$), comparable to the FRET ratio of 2.28 ± 0.12 in cells expressing Ven-linker-Ceru. However, cells expressing TEVp-tevS-Ven-tevS-Ceru recorded a much lower FRET ratio than cells expressing Ven-tevS-

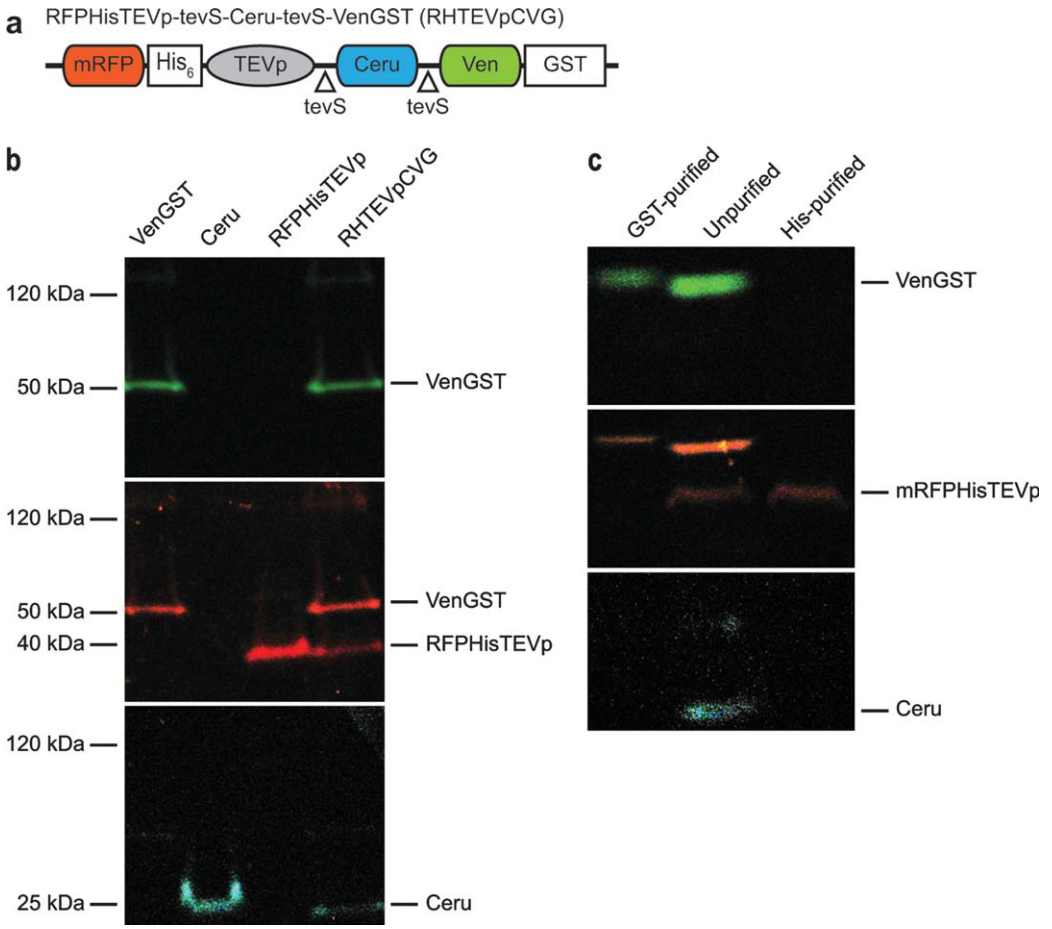

Figure 1. TEVp self-cleavage in *E. coli*. (a) Schematic of construct used in b and c. Cleavage occurs at the sites containing tevS (ENLYFQS). (b) SDS-PAGE analysis for post-translational products of the construct shown in a compared against constructs encoding VenGST, Ceru, and RFPHisTEVp individually. The three panels, from top to bottom, are pictures of the gel taken using Venus, mRFP, and Cerulean excitation/emission filters, respectively. Venus bands were detected under the mRFP filter due to cross excitation of Venus by mRFP excitation wavelength. The relative intensities of the bands are not indicative of the expression levels for their corresponding fluorescent proteins. (c) SDS-PAGE analysis of His-purified and GST-purified samples of the construct shown in a. The three panels follow the same pattern as described in (b). [Color figure can be viewed in the online issue, which is available at wileyonlinelibrary.com.]

Ceru (2.68 ± 0.07–1.56 ± 0.04), indicating a separation of the two fluorescent proteins facilitated by TEVp self-cleavage.

To further investigate TEVp self-cleavage, a fusion protein was constructed with three separable modules: RFPHisTEVp-tevS-Ceru-tevS-VenGST (RH TEVpCVG) [Fig. 1(a)]. The three reporter genes used (mRFP,[34] Cerulean and Venus) have distinctive spectral properties, allowing us to identify each subunit visually. TEVp itself was tethered to mRFP so that we could determine if it could excise itself through an adjacent tevS site. The polyhistidine tag (His) and glutathione *S*-transferase tag (GST) allowed purification of the modules and served as size fillers so that each module can be spatially distinguished on an electrophoretic gel. Lysate extracted from *E. coli* cells expressing this fusion protein was analyzed by sodium dodecyl sulfate polyacrylamide gel electrophoresis (SDS-PAGE). The major products were matched up against the controls and identified as RFPHisTEVp at ~40 kDa, Ceru at ~25 kDa, and VenGST at ~50 kDa [Fig. 1(b)]. We conducted both His-purification and GST-purification to show that individual modules can be isolated from RHTEVpCVG. The His-purified and GST-purified samples produced the same bands as RFPHisTEVp and VenGST, respectively [Fig. 1(c)]. While we expected to see some uncleaved (all three modules) and intermediate cleavage products (two modules) in both the lysate and purified samples, they did not appear on the gel, suggesting a complete or near complete cleavage of all TEV substrates between the modules.

Many cellular processes involve enzymatic or regulatory multiprotein complexes. It is often necessary to purify these complexes for biochemical studies. The conventional approach relies on *in vitro* reconstitution of proteins after they have been individually expressed and purified.[35] This is a tedious process and may not work in cases where chaperone

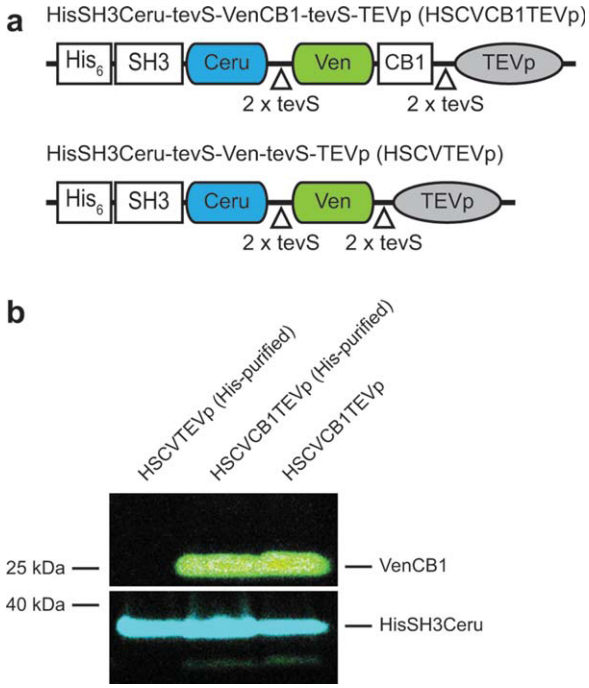

Figure 2. TEVp self-cleavage and subsequent purification of a binding complex. (a) Schematic of constructs used in (b). An additional tevS was added at the cleavage points compared to previous constructs. We anticipated that having a double tevS site may improve cleavage efficiency. (b) SDS-PAGE analysis of post-translational products of the constructs shown in a together with their His-purified samples, showing successful purification of the SH3-CB1 protein complex expressed from the TEVp self-cleavage system. The two panels, from top to bottom, are pictures of the gel taken using Venus and Cerulean excitation/emission filters, respectively. [Color figure can be viewed in the online issue, which is available at wileyonlinelibrary.com.]

proteins are required for proper complex formation. Here we demonstrate a utility of the TEVp self-cleavage system by expressing and purifying a two-protein complex from one TEVp self-cleavable fusion construct. In this case, the complex is reconstituted *in vivo* from the co-expressed proteins and only needs to be purified once. The construct we used, HisSH3-Ceru-tevS-VenCB1-tevS-TEVp [Fig. 2(a)], contained an N-terminal Src homology three domain of human Crk2 (SH3) and its binding peptide CB1. SH3 and CB1 were tagged with Cerulean and Venus respectively for visualization purposes. The post-cleavage products of HisSH3Ceru-tevS-VenCB1-tevS-TEVp were identified as HisSH3Ceru at ~30 kDa and VenCB1 at ~25 kDa by SDS-PAGE [Fig. 2(b)]. The same bands were produced after His-purification, suggesting that VenCB1 was co-purified together with HisSH3Ceru. However, the control construct HisSH3Ceru-tevS-Ven-tevS-TEVp in which CB1 was not present [Fig. 2(a)], only yielded the HisSH3Ceru band after His-purification. This experiment demonstrated the feasibly of purifying a protein complex from a TEVp self-cleavable fusion protein.

TEVp self-cleavage in mammalian cells

The TEVp self-cleavage of fusion proteins in mammalian cells expresses multiple proteins that were localized into different subcellular compartments. As with our work with *E. coli* cells, we utilized the distinctive fluorescent properties of Venus, Cerulean, and mRFP to noninvasively and simultaneously visualize the expression of up to three proteins in mammalian cells. When plasmids encoding Venus, Cerulean and mRFP were transfected into COS-7 cells, a uniform cytoplasmic and nucleoplasmic distribution was observed (data not shown). The size of these fluorescent proteins (~26 kDa) allowed them to cross nuclear pores. To confine each fluorescent protein in a specific cellular compartment, we introduced two localization motifs: (1) NLS: the nuclear localization sequence (RIRKKLR) derived from the p54 protein,[36] and (2) DAGR: the Cys1 domain of Protein Kinase C β-isoform, which translocates from the cytosol/nucleus to either the plasma or nuclear membrane upon phorbol 12,13-dibutyrate (PDBu) stimulation.[37,38] We built a nuclear localizing module by attaching two NLSs in tandem to the C-terminus of Cerulean (CeruNLS), and a membrane localizing module by attaching DAGR to the N-terminus of Venus (DAGRVen). To demonstrate TEVp self-cleavage and the subsequent subcellular targeting of the cleavage products, we constructed a four-module fusion protein TEVp-tevS-CeruNLS-tevS-DAGRVen-tevS-RFP (TEVpCNDVR) [Fig. 3(a)] which contained mRFP as well as the aforementioned CeruNLS and DAGRVen modules. The principle of differential localization is illustrated in Figure 3(b), showing the predicted targeting patterns of each module after cleavage.

After transfection of TEVpCNDVR in COS-7 cells, the subcellular localizations of the processed modules led to a distinctive fluorescence pattern as predicted. CeruNLS was observed only in the nucleus and nucleolus, whilst both DAGRVen and mRFP were evenly distributed in the entire cell (Fig. 4). The addition of 10 μ*M* of PDBu led to the migration of only DAGRVen to both plasma and nuclear membranes within 2 min (Fig. 4). Cytoplasmic and nuclear boundaries were confirmed by bright field microscopy. The same localization patterns were observed when plasmids encoding CeruNLS, DAGRVen and mRFP were individually transfected (data not shown). The control construct CeruNLS-tevS-DAGRVen-tevS-RFP, in which TEVp was not present, produced intense Cerulean, Venus, and mRFP fluorescence in the nucleus and was only able to localize to the nuclear membrane in response to 10 μ*M* of PDBu (Fig. 4). The display of all three fluorescent signals and the ability for DAGR to correctly respond to its stimulus confirm that all modules were properly folded and their functionality preserved. The apparent fluorescent

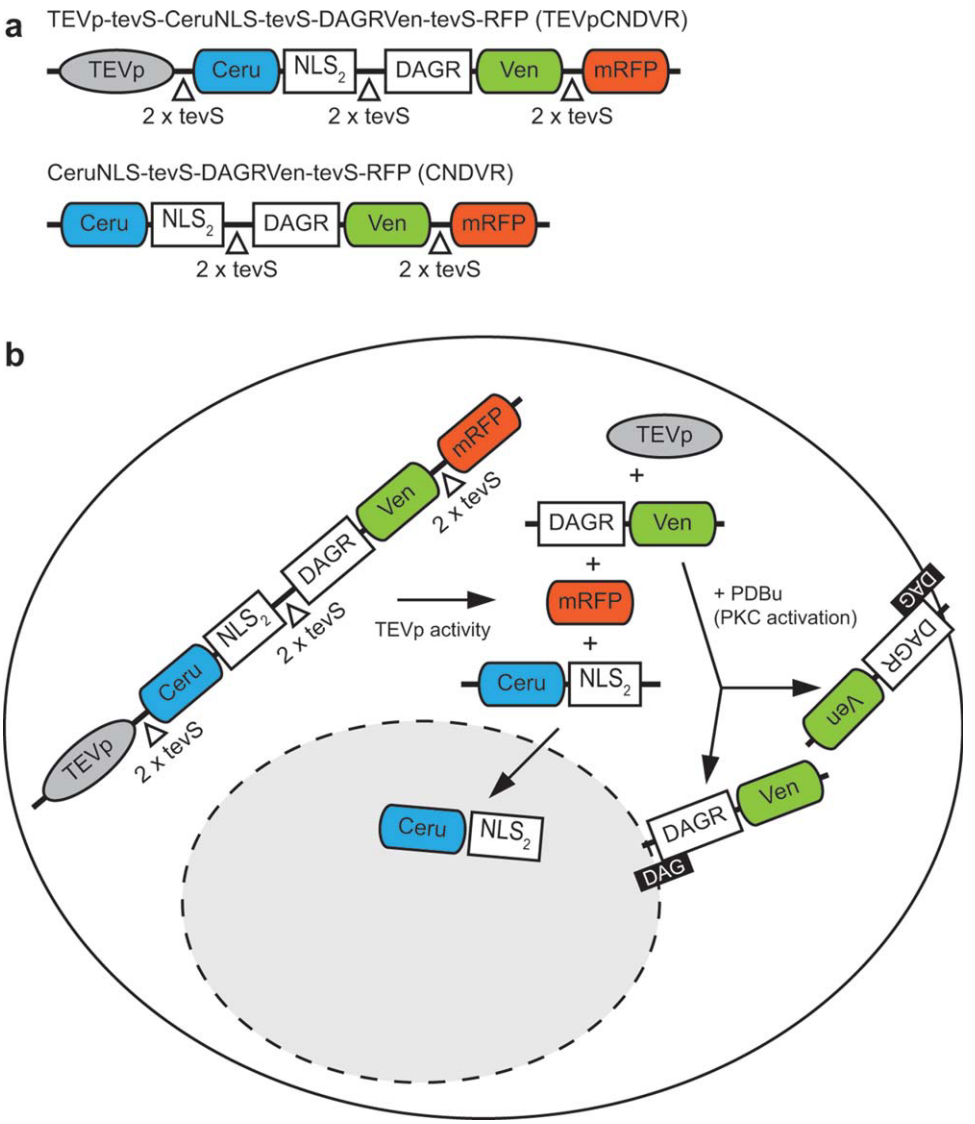

Figure 3. Differential localization of TEVp self-cleavage product in mammalian cells. (a) Schematics of the self-cleavage construct (TEVpCNDVR) and its non-cleavable control (CNDVR). (b) Conceptual illustration of what is expected to happen when the self-cleavage construct from (a) is expressed in eukaryotes. The CeruNLS module will enter the nucleus, while DAGRVen will bind to membrane-bound diglyceride (DAG) molecules upon PDBu stimulation. [Color figure can be viewed in the online issue, which is available at wileyonlinelibrary.com.]

intensities of both fusion constructs were comparable to that of the single gene constructs, suggesting that multiple genes can be transfected and expressed as a fusion without a significant change in expression levels. The localizations of the three fluorescent modules also appeared to be mutually exclusive, indicating that the cleavage was complete within the detection capability of our microscope. The transfection efficiency of the TEVpCNDVR fusion construct was ~14% following our standard transfection procedure (detailed comparison with the transfection efficiency of each of its modules can be found in Supporting Information Fig. S2). This low value is expected from constructs of its size, which may diminish its use in applications requiring high transfection efficiencies. However, it is possible to improve the transfection efficiency by optimizing DNA to liposome ratios or eliminate non-transfected cells by stable selection.

We repeated the differential localization experiment in HeLa and HEK-293 cells to show that TEVp self-cleavage is not cell-type specific. The expression of TEVpCNDVR was robust in both cell lines with identical localization patterns as in COS-7 cells (Fig. 5). The expression of the non-cleavable control construct was also identical. This highlights the advantage of having a self-contained cleavage system rather than relying on endogenous mechanisms for protein separation.

Stoichiometry of TEVp self-cleavage products

The single transfections of vectors encoding TEVp cleavage protein products yielded a consistent

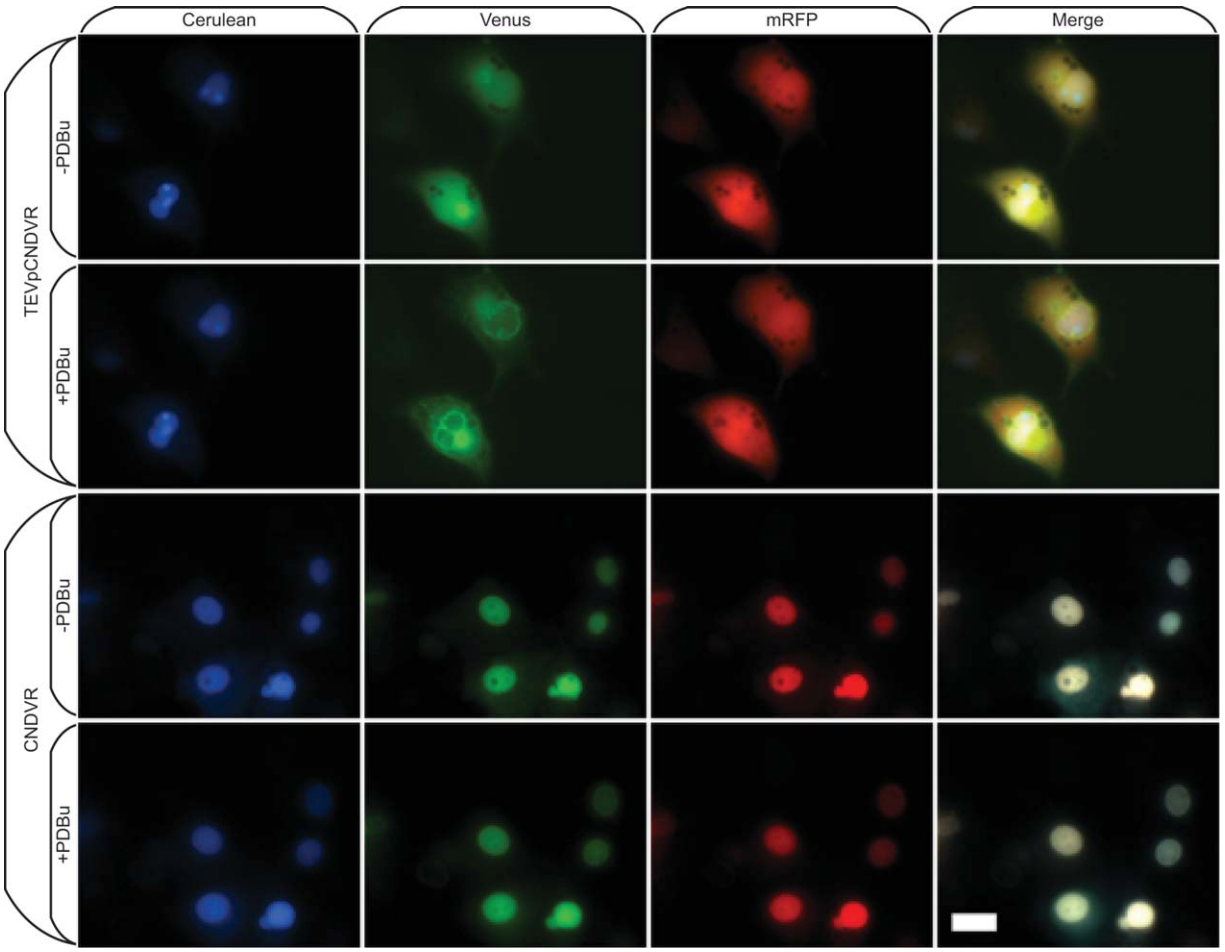

Figure 4. Images of live COS-7 cells expressing fusion constructs introduced in Figure 3(a). The top 2 rows shows the fluorescent patterns of the TEVp self-cleaving construct TEVp-tevS-CeruNLS-tevS-DAGRVen-tevS-RFP. The separate modules were distinctively localized, with only the DAGRVen module able to respond to PDBu by migrating to the membranes. The bottom two rows show the fluorescent patterns of the non-cleavable control CeruNLS-tevS-DAGRVen-tevS-RFP. It is clearly locked in the nucleus by the strong NLS signal. PDBu induced migration could be barely observed as intensely fluorescent pockets (of all three colors) were formed on the inner circumference of the nuclear membrane. Scale bar is 30 μm and applies to all panels. [Color figure can be viewed in the online issue, which is available at wileyonlinelibrary.com.]

stoichoimetry in contrast to a standard co-transfection of the separate protein products. To assess the stoichiometry of the cleavage products, we constructed three self-cleaving TEV fusions, each containing a combination of the Venus gene and the nuclear localizing CeruNLS gene in different ratios: TEVp-tevS-CeruNLS-tevS-Ven (TEVpCNV), TEVp-tevS-CeruNLS-tevS-Ven-tevS-Ven (TEVpCNVV), and TEVp-tevS-CeruNLS-tevS-CeruNLS-tevS-Ven (TEVp CNCNV) [Fig. 6(a)]. We anticipated that the molar ratios of Venus and CeruNLS protein products will be dictated by the frequency of representation of their genes on the vector constructs. For example, if the construct contains one CeruNLS gene to one Venus gene, the protein products should be expressed in equimolar ratio.

The transfection of the aforementioned constructs in COS-7 cells each resulted in an evenly distributed Venus signal and an intense nuclear localized Cerulean signal [Fig. 6(b)]. To estimate the expression levels of Ven and CeruNLS, we measured the fluorescent intensities of cytosolic Venus and nucleoplasmic Cerulean respectively. For the TEVpCNV construct, the ratio between CeruNLS and Venus (CeruNLS/Venus) was 1.03 ± 0.13 [Fig. 6(c)]. With an additional Venus gene compared to TEVpCNV, the TEVpCNVV construct doubled its Venus expression as shown by its CeruNLS/Venus ratio of 0.51 ± 0.04 [Fig. 6(c)]. Similarly, TEVpCNCNV doubled its CeruNLS expression with a CeruNLS/Venus ratio of 2.03 ± 0.35 [Fig. 6(c)]. To compare against the TEV fusion constructs, we examined cells co-transfected with Venus and CeruNLS. Unsurprisingly, Venus/CeruNLS expression ratio in the co-transfected cells was 0.77 ± 0.57, which was non-stoichiometric and extremely inconsistent across the population [Fig. 6(c)].

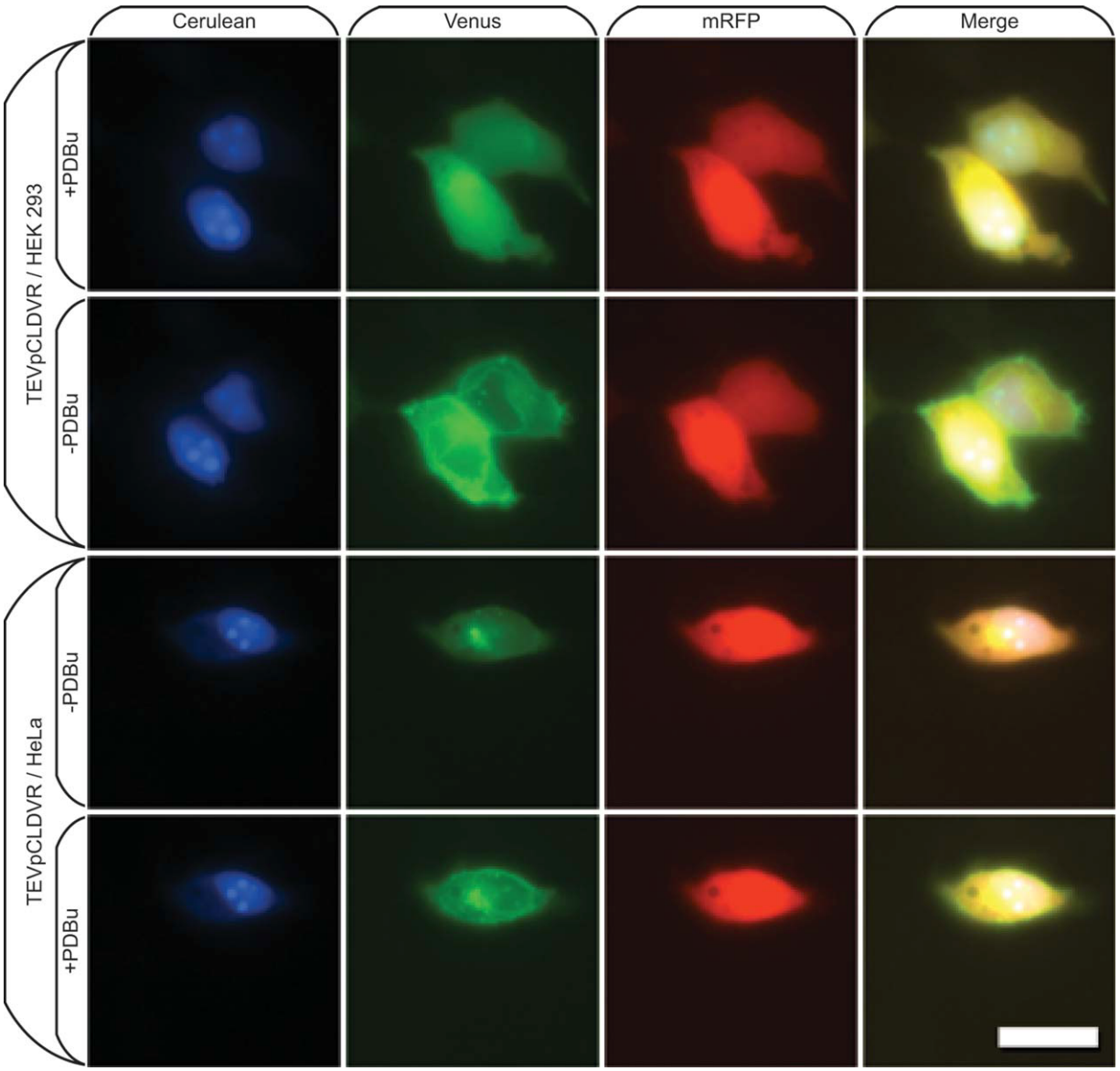

Figure 5. Images of live HEK-293 and HeLa cells expressing TEVp-tevS-CeruNLS-tevS-DAGRVen-tevS-RFP [introduced in Fig. 3(a)], showing identical localization patterns as COS-7 cells (Fig. 4). Scale bar is 30 μm and applies to all panels. [Color figure can be viewed in the online issue, which is available at wileyonlinelibrary.com.]

Conclusion

Borrowing from a theme in RNA viruses, we have described a single-vector multiple gene expression strategy by utilizing TEV protease self-cleavage. We have demonstrated the feasibility of this approach for robust expression of up to three genes in both bacterial (*E. coli*) and mammalian cells (COS-7, HeLa, and HEK-293). We have also verified that the stoichiometry of protein products was correlated with the frequency of appearance of their genes on the expression vector. We believe this work will find compelling applications where the expression stoichiometry is particularly important. For example, using this approach in structural biology, the reconstitution of protein complexes can happen within the bacterial host cell at the specific stoichiometry of its components. In synthetic signaling pathways, the response of synthetic system can be optimized on the relative concentration of multiple signaling proteins. Last, in the induction of pluripotent stem cells[3,8] or neuron cells,[39] it might be possible to improve the currently low induction rate of cells by a better control over the stoichiometry of the transcriptional factors.

Material and Methods

Construction of expression plasmids

All plasmids were built on the pTriEx-3 (Novagen) vector backbone which allows expression in both prokaryotes and eukaryotes (by a CMV promoter). Plasmids encoding TEV protease (TEVp), TEV substrate (tevS), fluorescent proteins (Cerulean,[40] Venus,[40] and mRFP[41]), purification tags (His[42] and

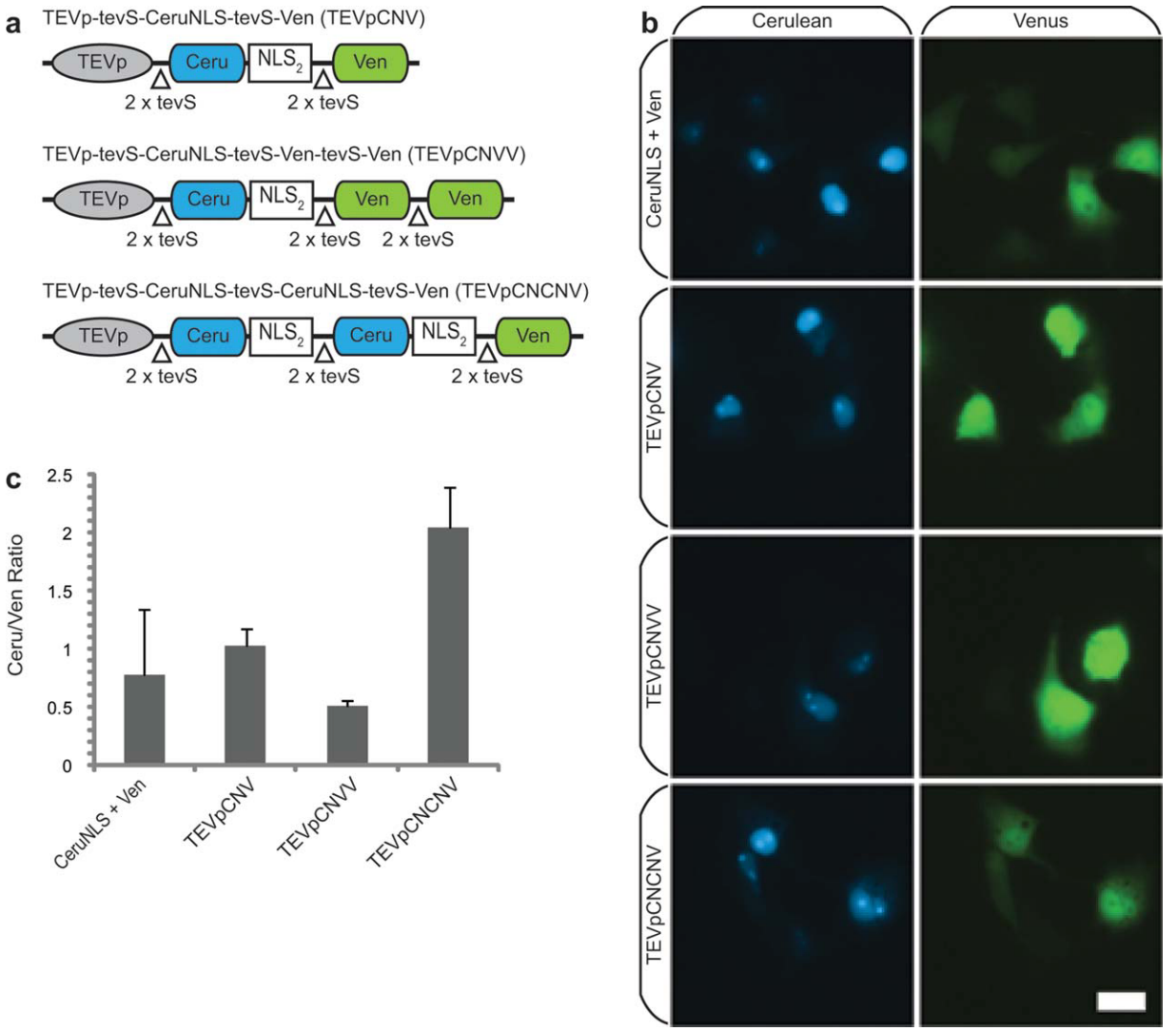

Figure 6. Stoichiometry of TEVp self-cleavage products. (a) Schematics of constructs used for (b) and (c). (b) Images of live COS-7 cells expressing each of the constructs shown in a. (c) CeruNLS/Venus expression ratios as represented by the ratio between nucleoplasmic Cerulean and cytoplasmic Venus fluorescence ($n = 40$). Error bars represent s.d. Scale bar is 30 μm and applies to all panels. [Color figure can be viewed in the online issue, which is available at wileyonlinelibrary.com.]

GST[42]), and localization signals (DAGR and NLS) were used as the fundamental building blocks for all fusion constructs. tevS and NLS were created by amplifying the Venus gene with custom primers (Invitrogen) containing tevS and NLS overhanging sequences. DAGR and TEVp were subcloned by polymerase chain reaction from published plasmids pRK1043 (Addgene)[27] and DAGR (Addgene),[38] respectively. All constructs contain flanking NcoI-SpeI and NheI-XhoI sites which allowed efficient recombination using the fluorescent cassette-based approach of Truong *et al.*[42]

Bacterial expression

DH5α competent cells (Invitrogen) were transformed with the plasmids and cultured overnight in Luria Broth (LB) supplemented with 100 μg/mL ampicillin at 37°C. The proteins were produced through leaky expression and extracted from the cells by sonication in Tris-NaCl buffer (50 n*M* Tris pH 7.5, 100 m*M* NaCl). The protein concentration in each lysate sample was normalized by fluorescence intensity observed under Illumatool Tunable Lighting System (Light Tools Research, Encinitas, CA). The lysate samples were diluted with Tris-NaCl buffer to arrive at a uniform fluorescence.

Affinity tag purifications and protein electrophoresis

Equal amounts of fluorescence-normalized lysates or purified protein solutions were mixed with NuPAGE LDS sample buffer (Invitrogen) before they were loaded on NuPAGE Novex 4–12% Bis-Tris precast polyacrylamide gels (Invitrogen) and ran on a Vertical Electrophoresis System (Thermo Scientific). His-tag purifications were performed using a His-Mag

Purification Kit (Novagen) following manufacturer's protocol. For GST-tag purifications, the lysate was mixed with GST sepharose beads (Novagen), washed several times and finally suspended in Tris-NaCl buffer. We did not elute the proteins from the GST sepharose beads because the commonly used glutathione elution buffer quenches Venus fluorescence. Instead, we loaded the beads suspension directly onto the polyacrylamide gel. Gels were viewed using Illumatool Tunable Lighting System, with 440/480 nm (excitation/emission) filters for Cerulean, 488/520 nm filters for Venus, and 540/580 nm filters for mRFP, to reveal only the fluorescent bands. Photographs of the fluorescent bands were taken by a Canon A350 Powershot camera. Contrast and brightness of the photographs were adjusted using Adobe Photoshop CS3 software.

Cell culture

COS-7, HeLa and HEK-293 cells were cultured as monolayers in Dulbecco's modified Eagle's medium (DMEM) (Invitrogen) supplemented with 10% fetal bovine serum (FBS) (Invitrogen), at 37°C in a humidified atmosphere containing 5% CO_2.

Imaging of transgene expression

Prior to transfection, cultured cells were passaged and incubated overnight as monolayers on 35 mm glass-bottom wells. Cells were transiently transfected with 1.6 μg of DNA for each construct using Lipofectamine 2000 (Invitrogen) according to the manufacturer's protocol. After overnight incubation, the monolayers were immersed in 1 mL phosphate buffered saline (PBS) and studied under a fluorescence microscope (Olympus) for fluorescence expression. 438/458, 500/535, and 580/630 nm excitation/emission filter pairs were used for Cerulean, Venus, and mRFP imaging respectively. To stimulate membrane localization of DAGR, 10 μ*M* of PDBu (Sigma-Alderich) was added. Images were captured by a CCD camera and processed with QEDInVivo software package.

Quantification of transgene expression

Using Image-Pro 6.0 software (MediaCybernetics), the relative amount of fluorescent proteins in a region of interest (X_{ROI}) was estimated by the following formula with the assumption that the cells were flat (2-dimensional):

$$X_{ROI} = I_{ROI} \times N_{ROI} \times \varepsilon \times \Phi \times T_{filler}. \quad (1)$$

The region of interest (ROI) for calculating Cerulean and Venus fluorescence were the nucleus and the cytoplasm respectively. I_{ROI} is the background corrected average pixel intensity within the ROI and N_{ROI} is the total number of pixels within the ROI. The relative brightness of each fluorescent protein is represented by the product of its extinction coefficient (ε) and quantum yield (Φ). T_{filter} is the transmission efficiency of the respective filter set in the microscope for each fluorescent protein. The ε, Φ and T_{filter} values for both Venus and Cerulean are listed in Supporting Information Table S1.

Acknowledgments

We thank J. Ge for constructing the TEVp and tevS plasmids and E. Mills for selecting a suitable NLS sequence.

References

1. Szymczak AL, Workman CJ, Wang Y, Vignali KM, Dilioglou S, Vanin EF, Vignali DAA (2004) Correction of multi-gene deficiency in vivo using a single 'self-cleaving' 2A peptide-based retroviral vector. Nat Biotechnol 22:589–594.
2. Bashor CJ, Helman NC, Yan S, Lim WA (2008) Using engineered scaffold interactions to reshape map kinase pathway signaling dynamics. Science 319:1539–1543.
3. Takahashi K, Yamanaka S (2006) Induction of pluripotent stem cells from mouse embryonic and adult fibroblast cultures by defined factors. Cell 126:663–676.
4. Villemure J-F, Savard N, Belmaaza A (2001) Promoter suppression in cultured mammalian cells can be blocked by the chicken β-globin chromatin insulator 5'HS4 and matrix/scaffold attachment regions. J Mol Biol 312:963–974.
5. Chen W-S, Chang Y-C, Chen Y-J, Chen Y-J, Teng C-Y, Wang C-H, Wu T-Y (2009) Development of a prokaryotic-like polycistronic baculovirus expression vector by the linkage of two internal ribosome entry sites. J Virol Methods 159:152–159.
6. Mizuguchi H, Xu Z, Ishii-Watabe A, Uchida E, Hayakawa T (2000) IRES-dependent second gene expression is significantly lower than cap-dependent first gene expression in a bicistronic vector. Mol Ther 1: 376–382.
7. Donnelly MLL, Luke G, Mehrotra A, Li X, Hughes LE, Gani D, Ryan MD (2001) Analysis of the aphthovirus 2A/2B polyprotein 'cleavage' mechanism indicates not a proteolytic reaction, but a novel translational effect: a putative ribosomal 'skip'. J Gen Virol 82:1013–1025.
8. Okita K, Nakagawa M, Hyenjong H, Ichisaka T, Yamanaka S (2008) Generation of mouse induced pluripotent stem cells without viral vectors. Science 322: 949–953.
9. Fang J, Qian J-J, Yi S, Harding TC, Tu GH, VanRoey M, Jooss K (2005) Stable antibody expression at therapeutic levels using the 2A peptide. Nat Biotechnol 23: 584–590.
10. Donnelly M, Gani D, Flint M, Monaghan S, Ryan M (1997) The cleavage activities of aphthovirus and cardiovirus 2A proteins. J Gen Virol 78:13–21.
11. de Felipe P, Luke GA, Hughes LE, Gani D, Halpin C, Ryan MD (2006) E unum pluribus: multiple proteins from a self-processing polyprotein. Trends Biotechnol 24:68–75.
12. de Felipe P, Luke GA, Brown JD, Ryan MD (2010) Inhibition of 2A-mediated lsquocleavagersquo of certain artificial polyproteins bearing *N*-terminal signal sequences. Biotechnol J 5:213–223.
13. de Felipe P, Ryan MD (2004) Targeting of proteins derived from self-processing polyproteins containing multiple signal sequences. Traffic 5:616–626.

14. Dougherty WG, Semler BL (1993) Expression of virus-encoded proteinases: functional and structural similarities with cellular enzymes. Microbiol Rev 57:781–822.
15. Allison R, Johnston RE, Dougherty WG (1986) The nucleotide sequence of the coding region of tobacco etch virus genomic RNA: Evidence for the synthesis of a single polyprotein. Virology 154:9–20.
16. Adams MJ, Antoniw JF, Beaudoin F (2005) Overview and analysis of the polyprotein cleavage sites in the family Potyviridae. Mol Plant Pathol 6:471–487.
17. Kapust RB, Tözsér J, Copeland TD, Waugh DS (2002) The P1′ specificity of tobacco etch virus protease. Biochem Biophys Res Commun 294:949–955.
18. Kapust RB, Waugh DS (2000) Controlled intracellular processing of fusion proteins by TEV protease. Protein Expr Purif 19:312–318.
19. Hartmann BM, Kaar W, Yoo IK, Lua LHL, Falconer RJ, Middelberg APJ (2009) The chromatography-free release, isolation and purification of recombinant peptide for fibril self-assembly. Biotechnol Bioeng 104:973–985.
20. Tubb MR, Smith LE, Davidson WS (2009) Purification of recombinant apolipoproteins A-I and A-IV and efficient affinity tag cleavage by tobacco etch virus protease. J Lipid Res 50:1497–1504.
21. Higuchi T, Uhlmann F (2005) Stabilization of microtubule dynamics at anaphase onset promotes chromosome segregation. Nature 433:171–176.
22. Pauli A, Althoff F, Oliveira RA, Heidmann S, Schuldiner O, Lehner CF, Dickson BJ, Nasmyth K (2008) Cell-type-specific TEV protease cleavage reveals cohesin functions in *Drosophila* neurons. Dev Cell 14: 239–251.
23. Sato M, Toda T (2007) Alp7/TACC is a crucial target in Ran-GTPase-dependent spindle formation in fission yeast. Nature 447:334–337.
24. Harder B, Schomburg A, Pflanz R, Küstner KM, Gerlach N, Schuh R (2008) TEV protease-mediated cleavage in Drosophila as a tool to analyze protein functions in living organisms. Biotechniques 44:765–772.
25. Marcos JF, Beachy RN (1997) Transgenic accumulation of two plant virus coat proteins on a single self processing polypeptide. J Gen Virol 78:1771–1778.
26. Shih Y-P, Wu H-C, Hu S-M, Wang T-F, Wang AH-J (2005) Self-cleavage of fusion protein in vivo using TEV protease to yield native protein. Protein Sci 14: 936–941.
27. Kapust RB, Tözsér J, Fox JD, Anderson DE, Cherry S, Copeland TD, Waugh DS (2001) Tobacco etch virus protease: Mechanism of autolysis and rational design of stable mutants with wild-type catalytic proficiency. Protein Eng 14:993–1000.
28. Phan J, Zdanov A, Evdokimov AG, Tropea JE, Peters HK, III, Kapust RB, Li M, Wlodawer A, Waugh DS (2002) Structural basis for the substrate specificity of tobacco etch virus protease. J Biol Chem 277: 50564–50572.
29. Rekas A, Alattia J-R, Nagai T, Miyawaki A, Ikura M (2002) Crystal structure of Venus, a yellow fluorescent protein with improved maturation and reduced environmental sensitivity. J Biol Chem 277: 50573–50578.
30. Rizzo MA, Springer GH, Granada B, Piston DW (2004) An improved cyan fluorescent protein variant useful for FRET. Nat Biotechnol 22:445–449.
31. Henrichs T, Mikhaleva N, Conz C, Elke D, Boyd D, Zelazny A, Bibi E, Ban N, Ehrmann M (2005) Target-directed proteolysis at the ribosome. Proc Natl Acad Sci USA 102:4246–4251.
32. Köhler F (2003) A yeast-based growth assay for the analysis of site-specific proteases. Nucleic Acids Res 31: e16.
33. Wehr MC, Laage R, Bolz U, Fischer TM, Grunewald S, Scheek S, Bach A, Nave K-A, Rossner MJ (2006) Monitoring regulated protein-protein interactions using split TEV. Nat Methods 3:985–993.
34. Campbell RE, Tour O, Palmer AE, Steinbach PA, Baird GS, Zacharias DA, Tsien RY (2002) A monomeric red fluorescent protein. Proc Natl Acad Sci USA 99: 7877–7882.
35. Tan S, Hunziker Y, Sargent DF, Richmond TJ (1996) Crystal structure of a yeast TFIIA/TBP/DNA complex. Nature 381:127–134.
36. Mizuno T, Okamoto T, Yokoi M, Izumi M, Kobayashi A, Hachiya T, Tamai K, Inoue T, Hanaoka F (1996) Identification of the nuclear localization signal of mouse DNA primase: nuclear transport of p46 subunit is facilitated by interaction with p54 subunit. J Cell Sci 109:2627–2636.
37. Oancea E, Teruel MN, Quest AFG, Meyer T (1998) Green fluorescent protein (GFP)-tagged cysteine-rich domains from protein kinase C as fluorescent indicators for diacylglycerol signaling in living cells. J Cell Biol 140:485–498.
38. Violin JD, Zhang J, Tsien RY, Newton AC (2003) A genetically encoded fluorescent reporter reveals oscillatory phosphorylation by protein kinase C. J Cell Biol 161:899–909.
39. Vierbuchen T, Ostermeier A, Pang ZP, Kokubu Y, Südhof TC, Wernig M (2010) Direct conversion of fibroblasts to functional neurons by defined factors. Nature 463:1035–1041.
40. Pham E, Chiang J, Li I, Shum W, Truong K (2007) A computational tool for designing FRET protein biosensors by rigid-body sampling of their conformational space. Structure 15:515–523.
41. Chiang J, Li I, Truong K (2006) Creation of circularly permutated yellow fluorescent proteins using fluorescence screening and a tandem fusion template. Biotechnol Lett 28:471–475.
42. Truong K, Khorchid A, Ikura M (2003) A fluorescent cassette-based strategy for engineering multiple domain fusion proteins. BMC Biotechnol 3:8.